EXPERIMENTAL DETERMINATION OF ADDED RESISTANCE OF BARNACLE FOULING ON SHIPS BY USING 3D PRINTED BARNACLES

Dogancan Uzun, University of Strathclyde, UK
Yansheng Zhang, University of Strathclyde, UK
Yigit Kemal Demirel, University of Strathclyde, UK
Osman Turan, University of Strathclyde, UK

3D printed artificial barnacles were attached on flat plates and towed over a range of Reynolds numbers in order to be able to calculate added resistance and power requirements of ships due to calcareous fouling. Since barnacle fouling occurs naturally it is possible to observe the barnacles in different sizes on any randomly selected ship surface. To model this condition three different barnacle sizes were selected and used to represent growing stages of the attached barnacles. The flat plates were covered with barnacles within a range of 10% to 50% area coverage respectively and towed over different speeds at the Kelvin Hydrodynamics Laboratory in the University of Strathclyde.
Frictional resistance coefficients and roughness function values were then calculated for each surface based on experimental results. Roughness effects of the given fouling conditions on the frictional resistances were then predicted for a containership ship using an in-house code developed based on boundary layer similarity law analysis. Added resistance diagrams were plotted using these predictions. Finally, the increase in the frictional resistance and powering penalties of the ship were predicted using the generated diagrams.

1. Introduction

Biofouling, which is a biological phenomenon can occur at anywhere in world seas and cause detrimental effects on ships performance. These kinds of organisms tend to attach to the underwater surface of a ship that can critically change the surface characteristics of ship hull. Although today many anti-fouling products exists, biofouling has not an exact solution since its quiet complicated, interdisciplinary as covering issues which are related to biology, chemistry and ship engineering, also it's an unstable problem depending on sea water properties.

As a repercussion of biofouling accumulation on ship, surface roughness increases resulting in additional frictional resistance. This subsequently causes extra fuel consumption, increase in Green House Gases (GHG) emissions and speed reductions. Major research has been done on effects of biofouling on frictional resistance, for instance, Schultz [19] has indicated that heavy calcareous fouling on naval frigate caused an 80% increase in total resistance at 15 knots speed. Another experimental study which is conducted by Andrewartha [1] showed a 99% increase in the drag coefficients of test plates due to biofilm formation in a recirculating water channel.

Although similar studies on biofouling effect on frictional resistance exist in literature, still there is no clear information which can be used by ship operators or engineers, who decide the exact time of ship's hull cleaning process. The person who makes sure that the ship operates in most efficient conditions, should be able to predict additional fuel consumption due to biofouling by performing routine observations of surface conditions through measuring dimensions of biofouling organisms like barnacles.

This is possible only if increase in friction coefficient C_F due to fouling is linked to the size of barnacles. Therefore the aim of this study is to establish a relation between the increase in C_F and the barnacle sizes and coverage area.

A series of towing tank experiments carried out using flat plates which are covered by artificial 3D printed barnacle bundles at the Kelvin Hydrodynamics Laboratory (KHL) of the University of Strathclyde. Coverage rates varied between 10% to 50% with 10% increments and three different barnacle sizes used in bundles design to realistically simulate barnacle accumulation regarding growth stages of barnacles. When frictional resistance coefficient (C_F) is known for both smooth and rough conditions, Granville's similarity theory can be used in order to scale frictional resistance up to large objects such as flat plates in ship length [9]. Some examples of the use of this method are given by Granville [10], Granville [11], Schultz [16], Schultz [17], Schultz [18], Flack and Schultz [8], Schultz et al. [20], Demirel et al. [5], Demirel [4] and Turan et al. [21].

This paper is organised as follows: Experimental facilities, model details and preparations within the study is presented in detail in Section 2 and 3, respectively. In Section 4, methodology is demonstrated while repeatability and uncertainty estimations for the conducted experiments are presented in Section 5. Frictional resistance coefficients for the surfaces and added resistance diagrams for ships in several lengths are presented in Section 6.Final remarks are presented in Section 7.

2. Experimental Facilities

The experiments were carried out at the Kelvin Hydrodynamics Laboratory (KHL) of the University of Strathclyde. The KHL test tank has dimensions of 76.0 m x 4.6 m x 2.5 m. The tank is equipped with a digitally-controlled towing carriage, state-of-the-art absorbing wave maker, and a highly effective sloping beach. The carriage has a velocity range of 0 – 5 m/s, with the velocity range used in these experiments kept between 1.5 and 3.6 m/s. Fresh water was used in the experiments, wherein the temperature of the water was monitored in order to be able to evaluate drag coefficients according to the temperature. The KHL towing tank and carriage has been shown in Figure 1.

Fig. 1 – The KHL Towing Tank and Carriage

Two transducers which are based on the Linear Variable Differential Transformer (LVDT) principle have been used to measure forces. One of the transducers was used on plates to control lateral force (lift force) and the other one was used for measuring drag force. Plates should be mounted parallel to the flow direction for getting accurate results therefore one transducer should measure the lift forces for being sure its zero at all time during the experiment. Before mounting the transducers on plates, calibration process was done by hanging weights on transducers' gauge and recording the voltage for each particular weight. These two transducers were calibrated separately across the expected load range.

3. Model Details and Preparations

Flat plates which used in the experiments were manufactured by KHL technicians using CNC machine. Metal type of flat plates is 304-stainless steel. The leading edge of plates rounded to 2.5 mm radius and sides of plates were grinded by 80 grit, 120 grit and 320 grit of sandpapers to mitigate extra drag due to the separation and roughness of plates. Figure 2 shows the dimensions of flat plates, locations of transducers, connections, towing direction and the general view of system.

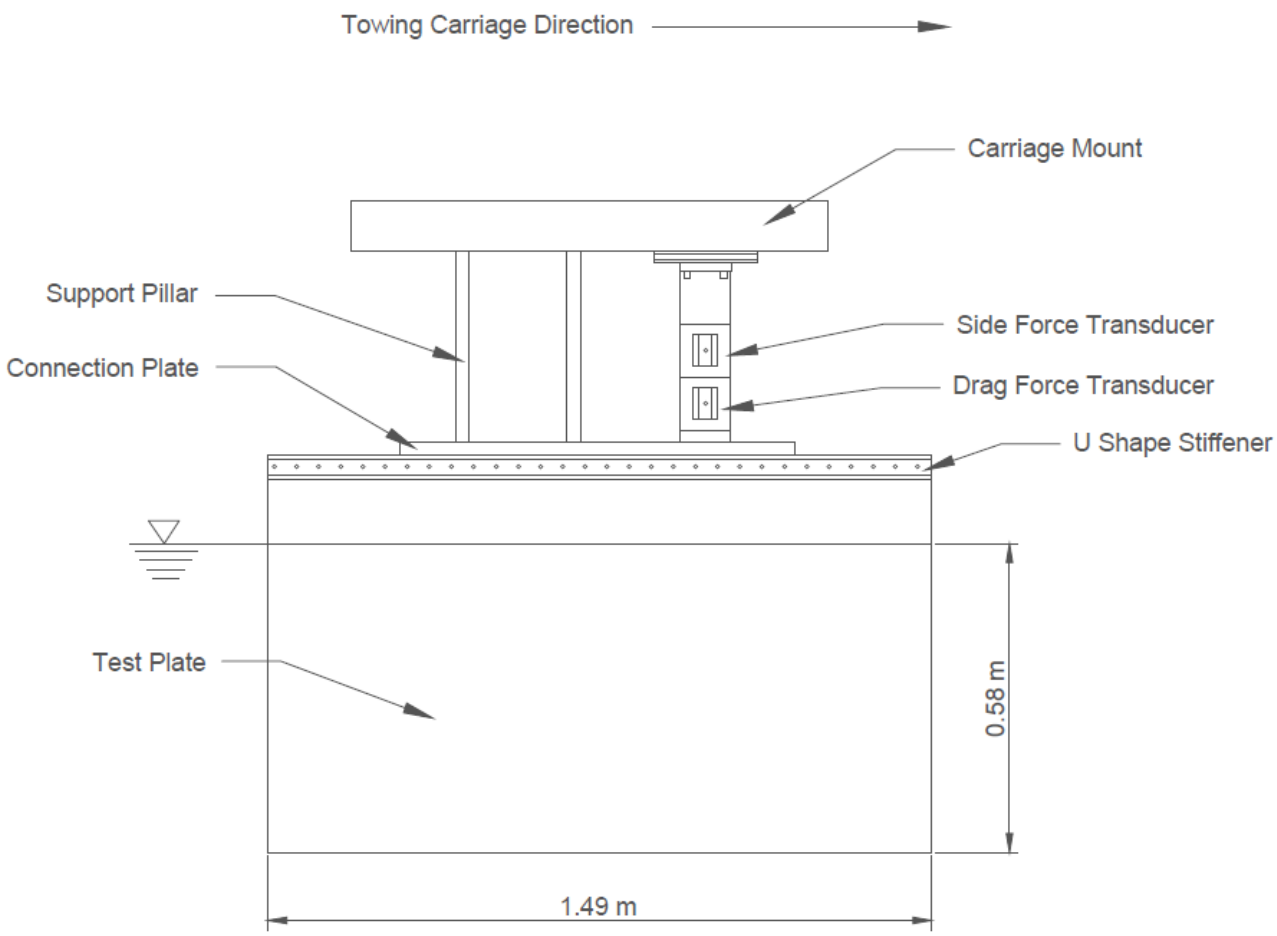

Fig. 2 – The Schematic of Flat plate test fixture

Artificial barnacles have been manufactured and used in this experiment using 3D scanning and printing technology. *Balanus improvisus* [3] or with its common name acorn barnacle, quite common barnacle specie especially in Europe, was selected to represent calcareous type macro fouling in this study. Its decided to represent barnacle type of bio-fouling on ships because of it is specie that can be seen commonly on ships and its ability of adaptation to different sea conditions such as salinity and temperature. After the selection of barnacle type, shape of barnacle was three dimensionally scanned and imported to computer aided modelling program. When a particular fouled ship surface area observed it's strongly possible to see barnacles in different size, the reason is this fouling is a biological phenomenon and these animals born, grow and die like as other animals. Observing different stages of barnacle growing on ship is not unusual therefore to simulate this situation, different sizes of barnacles were designed in modelling program by scaling original geometry. Types of barnacles have been defined as 3 type such as; Big, Medium and Small type and their dimensions have been shown in Table 1.

For the feasibility of experiment and getting rid of some uncertainty such as the distance between barnacles and settlement uniformity, models were prepared for manufacturing as bundles in the modelling program. Designed bundles can be seen in Figure 3.

Table 1 – Barnacle types and dimensions

Barnacle type	**Dimensions (diameter and height)**
Big	10 mm and 5 mm
Medium	5 mm and 2.5mm
Small	2.5 mm and 1.25mm

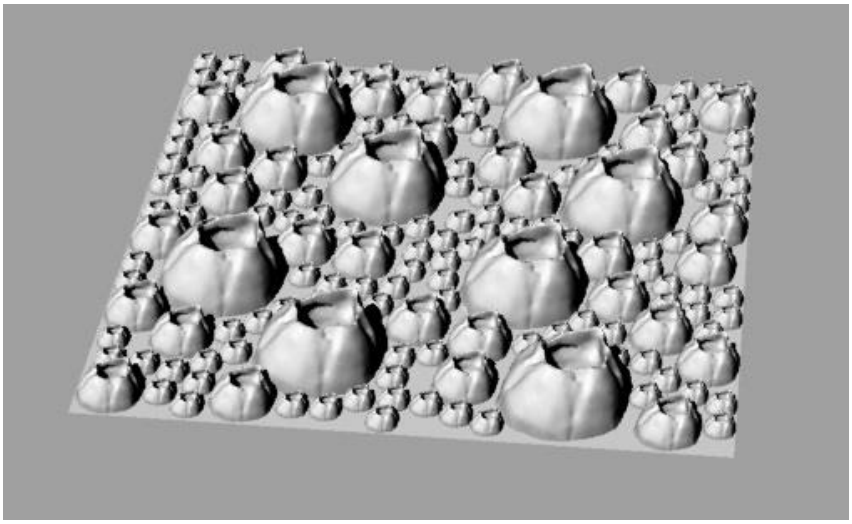

Fig. 3 – Picture of barnacle bundle

At first, a bare flat plate which named as Reference plate was towed to obtain a base line value that is necessary for being able to make comparison between other configurations and determining the exact drag increase with respect to uncovered plate. Bundles have been glued onto flat plates starting with 10% and increased to 50% area coverage with 10% increments. Location of bundles on the flat plate has been marked by using ASTM D6990-5 standards [2]. It should be noted that each configuration performs as a different surface and therefore each surface's coverage was towed at 10 different speeds. Following pictures illustrate the percentage of configurations on flat plates, respectively.

Fig. 4 – 10% coverage area of barnacles on flat plate

Fig. 5 – 20% area coverage of barnacles on flat plate

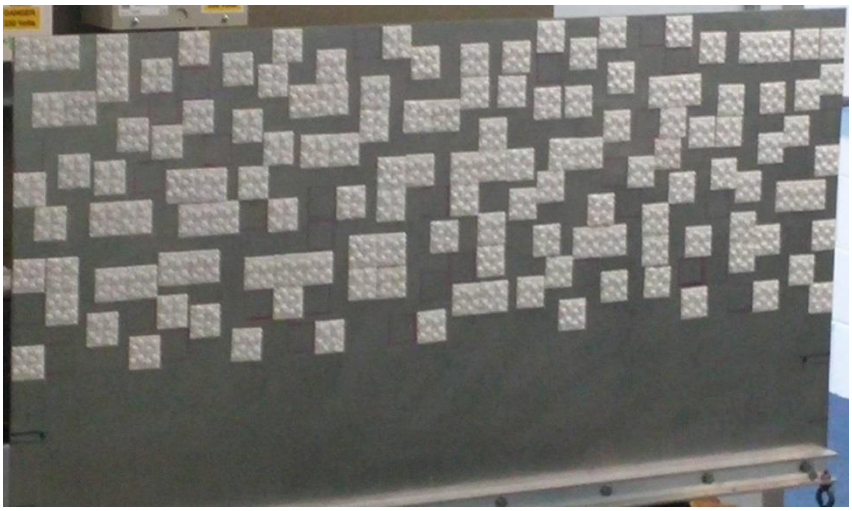

Fig. 6 – 40% area coverage of barnacles on flat plate

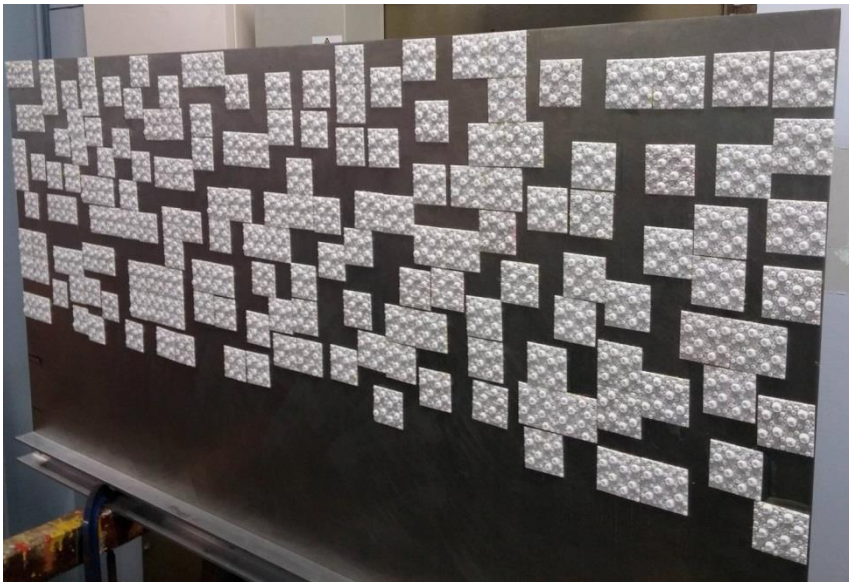

Fig. 7 – 50% area coverage of barnacles on flat plate

4. Methodology

4.1. Determination of Resistance Coefficients

Roughness experiment is not a new phenomenon therefore test methodology adapted from previous successful studies such as Schultz [18] and Demirel [4]. Experiments start with the alignment of flat plate, it's important to make accurate measures. Mounted plate was towed a number of times for measuring and monitoring side forces thanks to side transducer and if it's necessary required adjustments have been done on plate connection until to have zero side forces.

When ship moves at the surface of water, there will be resistance force which is composed of two different forces and these components were defined as frictional resistance and residual resistance respect to the ship resistance theory of William Froude. Basic equation can be seen at (1).

$$R_T = R_f + R_R \tag{1}$$

Frictional resistance is found by integrating tangential stresses of surface which drag the water due to viscous effects whereas residual resistance is a force that happens as a consequence of ship's movement based phenomena such as waves and Eddy effects which cause differences on pressure distributions all over the ship surface [23].

In this study thin flat plate, 0.5 mm thickness was used therefore the resistance due to form of model can be neglected and so the attached barnacles bundles will affect only the frictional resistance of flat plate.

To calculate the frictional resistance difference between the bare flat surface and the surface which covered with barnacles total resistance forces were obtained for each configuration within defined speed range.

$$R_T = \frac{1}{2}\rho S C_T V^2 \quad (2)$$

Where V, speed C_T, the total resistance coefficient, S the wetted surface area and ρ the density of water. With the assumptions as mentioned above Froude hypothesis turns into the equation at below as indicated as same in Schultz [19].

$$C_T = C_F(Re) + C_R(Fr) \quad (3)$$

As an explanation, total resistance coefficient is equal to sum of frictional resistance coefficient, C_F which is a function of Reynolds number, and residual resistance coefficient, C_R which is a function of Froude number. Since formula of ITTC 1957, well-known formula uses for calculating C_F , developed as a model-ship correlation line and not designed to represent the frictional resistance of plate therefore it has not been used in this study [24].

Schoenherr [15] conducted series of resistance experiments for surfaces in different lengths with the light of theoretical formula of Prandtl and von Karman which is indicated at below:

$$\frac{A}{\sqrt{C_f}} = \log_{10}(Re\ C_F) + M \quad (4)$$

As a consequence of his experiments, Schoenherr made a good fit to his experimental data by making M zero and A equal to 0.242, so the final well known Schoenherr formulation can be seen at below [24]:

$$\frac{0.242}{\sqrt{C_f}} = \log_{10}(Re\ C_F) \quad (5)$$

Instead of ITTC 1957 formula, as suggested at van Manen and van Oossanen [22], Schonherr friction line was used in terms of having accurate correlation with ship hulls which have different kind of roughness. Schoenherr friction line was used in previous similar studies such as Schultz [18] and Demirel [4].

The frictional resistance and residual resistance are resistance components that generate the total resistance as shown at Equation (3).To find the roughness effects on frictional resistance, C_F can be calculated by subtracting C_R from the C_T , under the assumption of roughness does not affect the residual resistance coefficient. When the C_R of reference plate calculated, C_F values of artificially roughened plates can be computed with the help of simple subtracting process as illustrated at following equations.

The required water properties such as water density and kinematic viscosity at different temperatures for basic resistance calculation were taken from ITTC Recommended Procedures of Fresh water and Sea water properties, report code 7.5-02-01-03 [14].

$$C_{R_s} = C_{T_s} - C_{F_s} \quad (6)$$

$$C_{R_s} = C_{R_r} \tag{7}$$

$$C_{F_r} = C_{T_r} - C_{R_r} \tag{8}$$

$$\frac{\left(C_{F_r} - C_{F_s}\right)}{C_{F_s}} x100 = \%\Delta C_F \tag{9}$$

$$\frac{\left(C_{T_r} - C_{T_s}\right)}{C_{T_s}} x100 = \%\Delta P_E \tag{10}$$

5. Repeatability and Uncertainty Estimations

The uncertainty estimates were done by using ITTC Recommended Procedures for Resistance, Uncertainty analysis and Example for Resistance test, report code 7.5-02-02-02 [13].Uncertainty is given in the form of general formula as the root of sum squares of the uncertainties of total bias and precision limits.

$$(U_x)^2 = (B_x)^2 + (P_x)^2 \tag{11}$$

Where U_x , total uncertainty, B_x total bias limit and P_x total precision limit. B_x occurs due to mismeasurement of devices used in experiment such as LVDT. It can be calculated by sum squares of multiplication of partial derivative of considered quantity with respect to variables and the bias which belong this variable.

$$(B_x)^2 = \left(\frac{\partial x}{\partial t} B_t\right)^2 + \left(\frac{\partial x}{\partial y} B_y\right)^2 + \left(\frac{\partial x}{\partial z} B_z\right)^2 \ldots \tag{12}$$

And x is a function of variables t, y and z as seen at below:

$$x = f(t, y, z) \tag{13}$$

The total precision limit P_x is caused by differences which can occur because of misalignment between the repeated tests. It can be calculated at following equations.

$$P(x_M) = \frac{KSDev}{\sqrt{M}} \tag{14}$$

$$P(x_S) = KSDev \tag{15}$$

Where M is the number of runs for which the precision limit is to be established, SDev is the standard deviation established by multiple runs and K is equal to 2 according to the methodology of ITTC (2002b). Formulation of SDev as below:

$$SDev = \left[\frac{\sum_{k=1}^{M}\left(x_k - x_{average}\right)^2}{M-1}\right]^{1/2} \tag{16}$$

The steps of uncertainty analysis can be found in ITTC [13]. In this experiment, the uncertainty analysis was carried out for two different speeds which represent low speed (1.857 m/s) and high speed (3.591 m/s) whose equal to Reynolds number of $\sim 2.6 \text{x} 10^6$ and $\sim 5 \text{x} 10^6$,respectively. The uncertainty limits for C_F were presented as values of bias, precision, total uncertainty and the change in percentage of whose quantities for all barnacle coverage configurations in two speeds.

The bias uncertainty in C_F ranged from ±7% at the lower Reynolds number to ±2% at the higher Reynolds number, whereas precision uncertainty in C_F ranged from ±3.4% at lower Reynolds number to ±0.54% at higher Reynolds number. The total uncertainty percentages in C_F are ±7% at low speed and ±2% at high speed. When the total uncertainty limits for drag coefficients compared to the previous study of Schultz [18], uncertainty limits at both studies are very close for both low and high Reynolds numbers.

6. Results

6.1. Frictional Resistance

Frictional resistance coefficients were calculated as explained in Section 4 at equations 6, 7, 8 and configuration comparisons were done against the reference plate. Figure 8 illustrates the frictional resistance coefficients of all test surfaces over a range of Reynolds number.

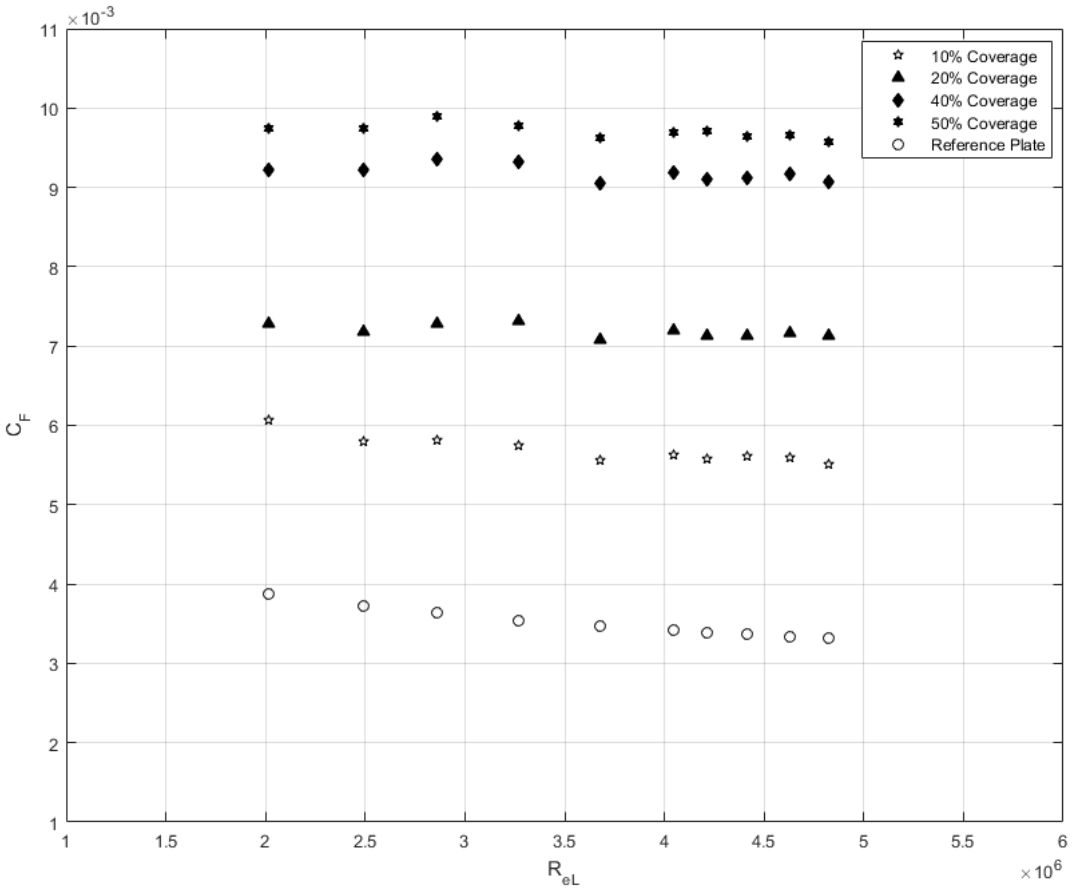

Fig. 8 – Frictional resistance coefficients of test surfaces

As seen from the Figure 8 and as expected, larger coverage area has bigger frictional resistance coefficient. Therefore 50% area coverage located at the top of Figure 8 followed by 40%, 20% and 10% coverage areas respectively. The changes in C_F values of the test surfaces with respect to the Reference plate are shown in Table 2.

Table 2 – Change ranges in frictional resistance coefficients (%) in speed range of 1.5 – 3.59 (m/s)

Configuration	Changes in C_F (%) in a speed range of (1.5 m/s-3.59 m/s)
10% Coverage	55.8-67.5
20% Coverage	88-115.2
40% Coverage	138.4-175
50% Coverage	151.9-189

It can be seen from the results in Table 2 that increases range in the C_F values of test surfaces are 55.8%-67.5% and 88%-115.2% for 10% and 20% coverage, whereas these values increased to 138.4%-175% and 151.9%-189% for 40% and %50 coverage configurations, respectively in a speed range of 1.5-3.59 (m/s). An interesting outcome from the table above is that, the percentage of increases in C_F values between the lower coverage configurations (10% and 20% coverage) are clearly higher than the increases between the higher coverage configurations (40% and 50% coverage).

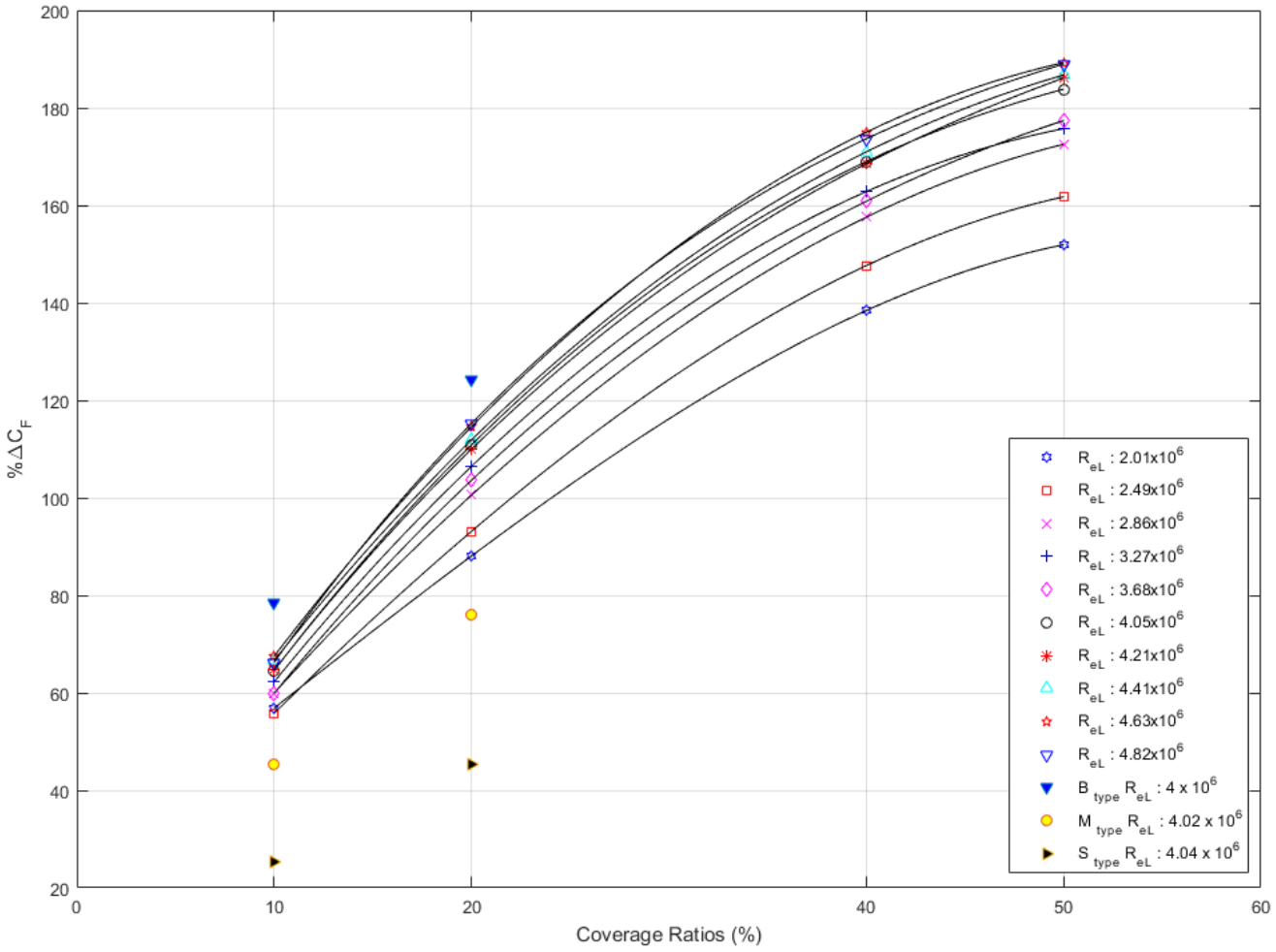

Fig. 9 – Percentage increases for frictional resistance coefficients respect to coverage ratios at different Reynolds numbers.

Also Figure 9 illustrates the percentage increases in the frictional resistance coefficients of different coverage ratios for varying Reynolds numbers. As can be seen in Figure 9 curves representing different Reynolds numbers get close to each other with ascending speed. This demonstrates the fact that after a certain threshold the frictional resistance becomes almost independent from Reynolds numbers as expected when the flow reaches the fully rough regime.

For comparison purposes, some of the results obtained by Demirel et al. [7] were also demonstrated in Figure 9. These are the increases in the frictional resistance of flat plates due to big sized (B-type), medium sized (M-type) and small sized (S-type) barnacles, respectively. It is important to note that in

this study we used the combination of these three different sizes of barnacles together. It can be seen in Figure 9 that the increases due to the mixed sized barnacles of the present study are close to the increases due to the big sized barnacles of Demirel et al. [7] at same Reynolds numbers. This shows that the presence of big-sized barnacles in the mixed configurations overweighs the existence of medium- and small-sized barnacles in the mixed configuration such that the increases due to the mixed configuration are almost similar to the increases due to the big-sized barnacles of Demirel et al. [7].

6.2. Prediction of the Roughness Effect of Barnacle Fouling on Added Resistance

The added resistance coefficients,ΔC_F, due to artificially fouled surfaces were calculated for 6 different imaginary ship length such as 10m, 30m, 50m, 100m, 150m and 250m thanks to help of an in-house code written based on principles which details of it can be found at study of Demirel et al. [7], Demirel et al. [6] and Grigson[12]. Obtained results, were employed in the code with considering roughness height (k) and ship length as inputs. Then the code calculates increases in C_F values of ship in any given roughness conditions for any critic ship speed which might be a cruise speed.

Third degree polynomial curves were then fitted on these calculated ΔC_F values and the diagrams which show ΔC_F trend respect to ship speeds were plotted. These diagrams have been created for each surface that experimentally measured in this study from 10% coverage to 50% coverage.

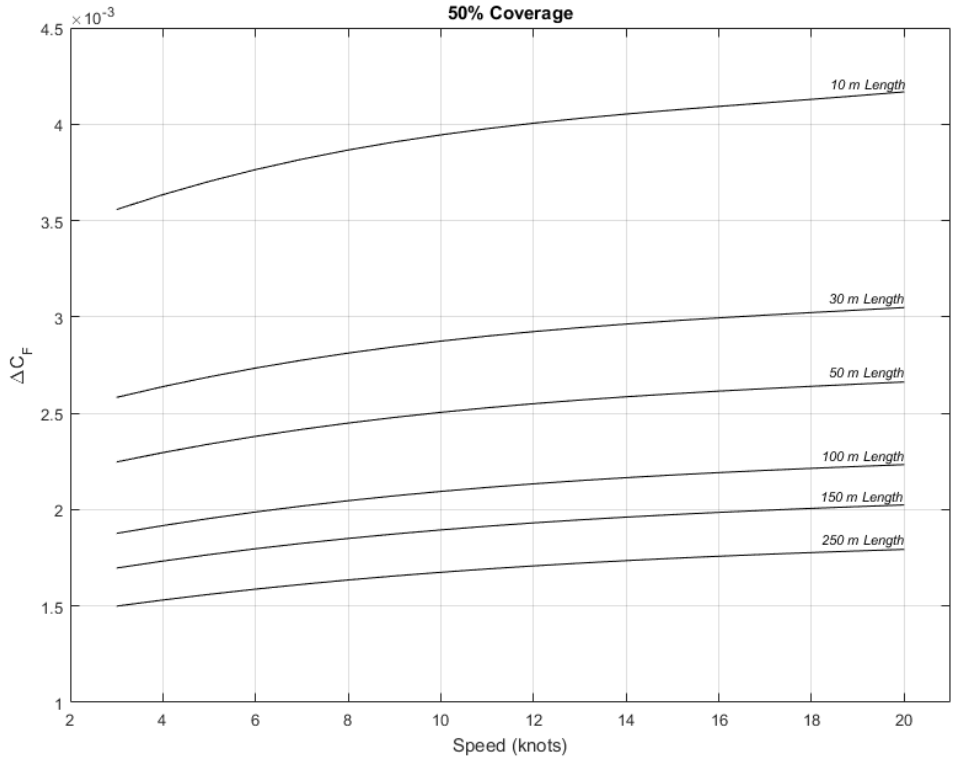

Fig. 10 – Added resistance diagrams for ships in the condition of 50% area coverage.

It's clearly seen form the each four diagrams roughness has an effect on frictional resistance of ships regarding to coverage area, characteristics of ship and speed. As expected, added frictional resistance is directly proportional with the ship speed therefore when the ship speed increase frictional resistance

will increase. It can be seen from each diagram when the curves inspected, the rate of increase at low speeds is higher than the increase at high speed. All diagrams show that length of ship is a significant parameter which affects the additional friction resistance and under the same roughness condition shorter ships are exposed to greater frictional resistance when compare to longer one. Respect to belief of authors this study can conduct a mission to be used as a simple and practical added resistance prediction reference by the ship operators for the ships which has barnacle fouling conditions in different area coverage.

6.3. Prediction of the Roughness Effect of Barnacle Fouling on Effective Power

A ship, 180 m length has been selected to be used as an example in these different roughness configurations at ship speed of 20 knots. Calculated ΔC_F values for 180 m bulk carrier are used with C_{TS} values of bulk carrier as indicated in Equation 10 to obtain ΔP_E values. Figure 11 illustrates the increases in frictional resistance and the effective power of the 180 m bulk carrier ship at a design speed of 20 knots.

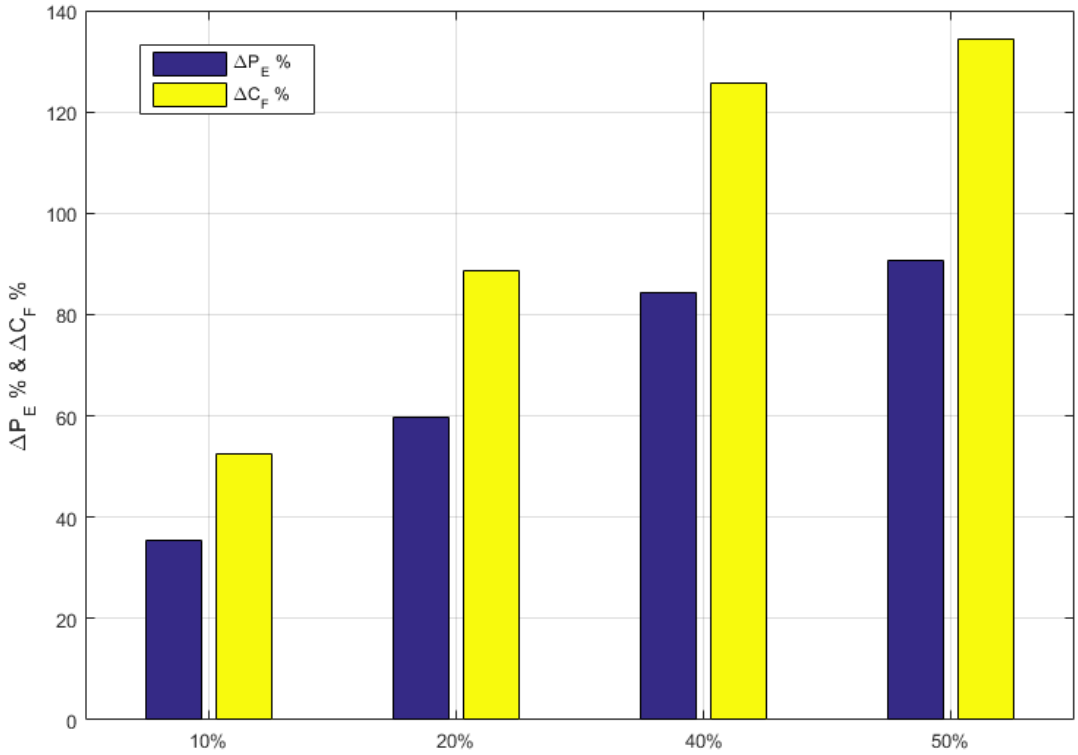

Fig. 11 – Percentage increases in C_F values and P_E values of 180m bulk carrier ship with respect to the smooth hull condition.

The percentage increases in C_F and P_E values of 180m ship due to barnacle fouling at ship speed of 20 knots predicted as 52.4% and 35.3% for 10% area coverage, 88.7% and 59.7% for %20 area coverage, 125.6% and 84.4 for 40% area coverage lastly 134.5% and 90.55% for 50% area coverage.

7. Discussion and Conclusions

By using 3D printing technology an experiment has been conducted to gain a practical and useful insight into the effect of barnacle fouling on ship resistance and powering. As illustrated in Section 3 plates were covered with artificial barnacles of different area coverage and towed in order at the KHL of the University of Strathclyde. Measured drag coefficients were then scaled to ship length to obtain the added resistance and effective power values for ship.

From the study, plotted diagrams can be seen as useful outcome for ship operators so that they provide an opportunity to make an accurate added resistance prediction possible for under the circumstances of any observed current fouled area coverage at several ship speeds.

The paper shows that capability to use 3D technology would create a chance to have a systematic way to understand the effect of fouling not only for barnacle fouling but also slime and algae type fouling. This would help us to generate new roughness functions and added resistance diagrams for the ships which have other type of biofouling.

8. Nomenclature

k	roughness length scale
ρ	density
ν	kinematic viscosity
L	plate length
S	wetted surface area
V	speed
R_{eL}	Reynolds number of plate
Fr	Froude number
R_e	Reynolds number
R_T	total resistance
R_F	frictional resistance
R_R	residuary resistance
P_E	effective power
C_T	total resistance coefficient
C_F	frictional resistance coefficient
C_R	residuary resistance coefficient
C_{T_s}	total resistance coefficient in smooth condition
C_{F_s}	frictional resistance coefficient in smooth condition
C_{R_s}	residuary resistance coefficient in smooth condition
C_{T_R}	total resistance coefficient in rough condition
C_{F_R}	frictional resistance coefficient in rough condition
C_{R_R}	residuary resistance coefficient in rough condition
ΔC_F	added resistance coefficient due to surface roughness
ΔP_E	increase in effective power due to surface roughness

9. References

1. Andrewartha, J., Perkins, K., Sargison, J., Osborn, J., Walker, G., Henderson, A., & Hallegraeff, G. (2010). Drag force and surface roughness measurements on freshwater biofouled surfaces. Biofouling, 26(4), 487-496. doi:10.1080/08927014.2010.482208
2. ASTM-D6990-05. (2011). Standard Practice for Evaluating Biofouling Resistance and Physical Performance of Marine Coating Systems. doi:10.1520/D6990-05R11
3. Darwin, C. R. 1854. A monograph on the sub-class Cirripedia, with figures of all the species. The Balanidæ, (or sessile cirripedes); the Verrucidæ, etc. etc. etc. London: The Ray Society. Volume 2.
4. Demirel, Y. K. (2015). Modelling the roughness effects of marine coatings and biofouling on ship frictional resistance. (PhD Thesis), University of Strathclyde.
5. Demirel, Y. K., Khorasanchi, M., Turan, O., & Incecik, A. (2013). On the importance of antifouling coatings regarding ship resistance and powering. Paper presented at the 3rd International Conference on Technologies, Operations, Logistics and Modelling for Low Carbon Shipping, London/UK.
6. Demirel, Y. K., Turan, O., & Incecik, A. (2017). Predicting the effect of biofouling on ship resistance using CFD. Applied Ocean Research, 62, 100-118. doi:http://dx.doi.org/10.1016/j.apor.2016.12.003
7. Demirel, Y. K., Uzun, D., Zhang, Y., Fang, H.-C., Day, A. H., & Turan, O. (2017). Effect of barnacle fouling on ship resistance and powering. *Biofouling*, 1-16. doi:10.1080/08927014.2017.1373279
8. Flack, K., & Schultz, M. (2010). Frictional drag measurements for pitted surface roughness. Paper presented at the APS Division of Fluid Dynamics Meeting Abstracts.
9. Granville, P. S. (1958). The frictional resistance and turbulent boundary layer of rough surfaces. Journal of Ship Research, 2, 52-74.
10. Granville, P. S. (1982). Drag-Characterization Method for Arbitrarily Rough Surfaces by Means of Rotating Disks. Journal of Fluids Engineering, 104(3), 373-377. doi:10.1115/1.3241854
11. Granville, P. S. (1987). Three indirect methods for the drag characterization of arbitrarily rough surfaces on flat plates. Journal of Ship Research, 31(1), 70-77.
12. Grigson, C. (1992). Drag losses of new ships caused by hull finish. Journal of Ship Research, 36(2), 182-196.
13. ITTC. (2002). Uncertainty Analysis, Example for Resistance Test. ITTC Recommended Procedures and Guidelines, Procedure 7.5-02-02-02, Revision 01. Retrieved from http://www.engr.mun.ca/veitch/ittc-uncertainty-resistance.pdf
14. ITTC. (2011). Fresh Water and Seawater Properties. ITTC Recommended Procedures and Guidelines, Procedure 7.5-02-01-03, Revision 02. Retrieved from https://ittc.info/media/1215/75-02-01-03.pdf
15. Schoenherr, K. E. (1932). Resistances of flat surfaces moving through a fluid. Transactions of SNAME, 40, 279-313.
16. Schultz, M. P. (1998). The Effect of Biofilms on Turbulent Boundary Layer Structure. (PhD Thesis), Florida Institute of Technology.
17. Schultz, M. P. (2002). The relationship between frictional resistance and roughness for surfaces smoothed by sanding. Journal of Fluids Engineering, 124(2), 492-499.
18. Schultz, M. P. (2004). Frictional resistance of antifouling coating systems. Journal of Fluids Engineering, 126(6), 1039-1047.

19. Schultz, M. P. (2007). Effects of coating roughness and biofouling on ship resistance and powering. Biofouling, 23(5), 331-341. doi:10.1080/08927010701461974
20. Schultz, M. P., Bendick, J. A., Holm, E. R., & Hertel, W. M. (2011). Economic impact of biofouling on a naval surface ship. Biofouling, 27(1), 87-98. doi:10.1080/08927014.2010.542809
21. Turan, O., Demirel, Y. K., Day, S., & Tezdogan, T. (2016). Experimental Determination of Added Hydrodynamic Resistance Caused by Marine Biofouling on Ships. Transportation Research Procedia, 14, 1649-1658. doi:http://dx.doi.org/10.1016/j.trpro.2016.05.130
22. van Manen, J. D., van Oossanen, P. (1988). Resistance. In: Lewis, E.V. (ed.). Principles of Naval Architecture. Second Revision. Volume II: Resistance, Propulsion and Vibration. Jersey City, NJ: The Society of Naval Architects and Marine Engineers.
23. Woods Hole Oceanographic Institution. (1952). Marine Fouling and Its Prevention. Annapolis, Maryland: United States Naval Institute.